
**RADIATION EFFECTS RESEARCH AND DEVICE
EVALUATION**

Clay Mayberry

4 April 2012

Final Report

APPROVED FOR PUBLIC RELEASE; DISTRIBUTION IS UNLIMITED.



**AIR FORCE RESEARCH LABORATORY
Space Vehicles Directorate
3550 Aberdeen Ave SE
AIR FORCE MATERIEL COMMAND
KIRTLAND AIR FORCE BASE, NM 87117-5776**

DTIC COPY NOTICE AND SIGNATURE PAGE

Using Government drawings, specifications, or other data included in this document for any purpose other than Government procurement does not in any way obligate the U.S. Government. The fact that the Government formulated or supplied the drawings, specifications, or other data does not license the holder or any other person or corporation; or convey any rights or permission to manufacture, use, or sell any patented invention that may relate to them.

This report was cleared for public release by the 377 ABW Public Affairs Office and is available to the general public, including foreign nationals. Copies may be obtained from the Defense Technical Information Center (DTIC) (<http://www.dtic.mil>).

AFRL-RV-PS-TR-2012-0023 HAS BEEN REVIEWED AND IS APPROVED FOR PUBLICATION IN ACCORDANCE WITH ASSIGNED DISTRIBUTION STATEMENT

//signed//
CLAY MAYBERRY
Program Manager

//signed//
B. SINGARAJU, Ph.D.
Deputy Chief, Spacecraft Technology Division
Space Vehicles Directorate

This report is published in the interest of scientific and technical information exchange, and its publication does not constitute the Government's approval or disapproval of its ideas or findings.

REPORT DOCUMENTATION PAGE

Form Approved
OMB No. 0704-0188

Public reporting burden for this collection of information is estimated to average 1 hour per response, including the time for reviewing instructions, searching existing data sources, gathering and maintaining the data needed, and completing and reviewing this collection of information. Send comments regarding this burden estimate or any other aspect of this collection of information, including suggestions for reducing this burden to Department of Defense, Washington Headquarters Services, Directorate for Information Operations and Reports (0704-0188), 1215 Jefferson Davis Highway, Suite 1204, Arlington, VA 22202-4302. Respondents should be aware that notwithstanding any other provision of law, no person shall be subject to any penalty for failing to comply with a collection of information if it does not display a currently valid OMB control number. **PLEASE DO NOT RETURN YOUR FORM TO THE ABOVE ADDRESS.**

| | | | | | | |
|---|------------------------------------|-------------------------------------|---------------------------------------|----------------------------|---|----|
| 1. REPORT DATE (DD-MM-YY) 04-04-2012 | | | 2. REPORT TYPE Final Report | | 3. DATES COVERED (From - To) 01 Oct 2003 – 01 Jan 2012 | |
| 4. TITLE AND SUBTITLE Radiation Effects Research and Device Evaluation | | | | | 5a. CONTRACT NUMBER | |
| | | | | | 5b. GRANT NUMBER | |
| | | | | | 5c. PROGRAM ELEMENT NUMBER 62601F | |
| 6. AUTHOR(S) Clay Mayberry | | | | | 5d. PROJECT NUMBER 4846 | |
| | | | | | 5e. TASK NUMBER PPM00004448 | |
| | | | | | 5f. WORK UNIT NUMBER EF002007 | |
| 7. PERFORMING ORGANIZATION NAME(S) AND ADDRESS(ES) Air Force Research Laboratory Space Vehicles Directorate 3550 Aberdeen Ave, SE Kirtland AFB, NM 87117-5776 | | | | | 8. PERFORMING ORGANIZATION REPORT NUMBER CHI'N'TX/RU/VT/4234/2245 | |
| 9. SPONSORING / MONITORING AGENCY NAME(S) AND ADDRESS(ES) | | | | | 10. SPONSOR/MONITOR'S ACRONYM(S) AFRL/RVSE | |
| | | | | | 11. SPONSOR/MONITOR'S REPORT NUMBER(S) | |
| 12. DISTRIBUTION / AVAILABILITY STATEMENT Approved for public release; distribution is unlimited. (377ABW-2012-0399, dtd 2 April 2012) | | | | | | |
| 13. SUPPLEMENTARY NOTES | | | | | | |
| 14. ABSTRACT The purpose of this basic research effort was to develop a systematic approach to determining radiation sensitivity in organic semiconductor based devices, including particularly photo-voltaics but also evaluating and characterizing organic based diodes, transistors including field effect devices and basic structures. The scope of the effort included both an experimental component that included application of accelerated testing with both ionizing radiation and elevated temperatures, as well as a modeling component to understand and confirm degradation mechanisms. The findings included the discovery that carrier lifetimes were unaffected by ionizing radiation but degradation manifested itself in the development of an internal potential that tended to reduce efficiency of the organic photovoltaic devices tested. This conclusion, along with any recommendations, will be utilized by device fabricators to attempt a mitigation scheme. | | | | | | |
| 15. SUBJECT TERMS Organic semiconductor radiation testing, photovoltaics, organic transistors, organic diodes | | | | | | |
| 16. SECURITY CLASSIFICATION OF: | | | 17. LIMITATION OF ABSTRACT | 18. NUMBER OF PAGES | 19a. NAME OF RESPONSIBLE PERSON Clay Mayberry | |
| a. REPORT Unclassified | b. ABSTRACT Unclassified | c. THIS PAGE Unclassified | | | Unlimited | 20 |

(This page intentionally left blank)

Table of Contents

| | |
|---|-----------|
| 1.0 RESEARCH OBJECTIVES | 1 |
| 2.0 SUMMARY OF FY11 PROGRESS | 1 |
| 3.0 BACKGROUND | 1 |
| 4.0 EXPERIMENT | 1 |
| <i>4.1 New Radiation Data</i> | <i>2</i> |
| <i>4.2 Dose Rate Effect</i> | <i>4</i> |
| <i>4.3 Relationship between Charge and Accumulated Dose</i> | <i>5</i> |
| <i>4.4 Ancillary interface modification studies</i> | <i>6</i> |
| 5.0 MODELLING | 7 |
| <i>5.1 Simulations (General Information)</i> | <i>7</i> |
| <i>5.2 Open-circuit voltage simulations (Pre-radiation)</i> | <i>8</i> |
| <i>5.3 Relaxation Time Simulations (Pre-radiation)</i> | <i>8</i> |
| <i>5.4 Charging Simulations</i> | <i>10</i> |
| 6.0 CONCLUSIONS | 11 |
| REFERENCES | 13 |

List of Figures

| | |
|---|----|
| Figure 1. The effect of radiation on photo-induced carrier relaxation/recombination time constant (τ)..... | 2 |
| Figure 2. Effect of accumulated radiation on V_{oc} for different weight ratios of P3HT to PCBM..... | 3 |
| Figure 3. V_{oc} plotted as a function of weight ratio..... | 3 |
| Figure 4. V_{oc} versus irradiation time up to a cumulated incident dose ~ 500 krad(SiO ₂). Subsequently the device was allowed to relax ($t > 50$ min)..... | 4 |
| Figure 5. ΔV_{oc} plotted as a function of accumulated dose for 1:1 samples. Attenuation factor is being accounted for in the dose rates. All dose rates are in krad/min (SiO ₂). | 5 |
| Figure 6. Charge plotted as a function of accumulated dose. | 6 |
| Figure 7. Experimental results of the relaxation time measurements (logarithmic scale) of 1:1 P3HT: PCBM samples with different interfaces at the cathode. | 6 |
| Figure 8. Predicted V_{oc} as a function of the carrier injection rate for different recombination methods; (\square) no SRH or Langevin, (\blacklozenge) Langevin only, (\blacktriangledown) $\tau_{SRH} = 10^{-6}$ s, (Δ) $\tau_{SRH} = 10^{-7}$ s, and (\bullet) $\tau_{SRH} = 10^{-8}$ s. | 9 |
| Figure 9. The lifetime as a function of V_{oc} for different recombination methods; (\square) no SRH or Langevin, (\blacklozenge) Langevin only, (\blacktriangledown) $\tau_{SRH} = 10^{-6}$ s, (Δ) $\tau_{SRH} = 10^{-7}$ s, and (\bullet) $\tau_{SRH} = 10^{-8}$ s. | 10 |
| Figure 10. The simulated change in V_{oc} due to the presence of the trapped hole density; (\square) the V_{oc} with zero charge is 0.33 V, (\circ) 0.40 V, and (\bullet) 0.45 V..... | 11 |
| Figure 11. The simulated carrier relaxation time as a function of V_{oc} : (Δ) the incident light level was adjusted to vary V_{oc} , (\square , \circ , and \bullet) increasing trapped hole density near the anode with the initial $V_{oc} = 0.33V$, $0.40V$, and $0.45 V$ respectively..... | 11 |

1.0 RESEARCH OBJECTIVES

We had two objectives for this effort. First, we wanted to develop a systematic approach to determine radiation sensitivity in organic semiconductor based devices, using photo-voltaic devices as a matter of expediency. Our second objective was to apply the test and modeling techniques to characterize an array of organic based devices (FETs, photo-cells, etc.) developed through other projects.

2.0 SUMMARY OF FY11 PROGRESS

In FY11 we made significant advances in the understanding and modeling of radiation effects in organic semiconductor devices. We used device modeling to simulate the behavior of P3HT:PCBM based photo-cells, we developed a qualitative description of the open-circuit voltage (V_{oc}) variations and photo-induced carrier relaxation/recombination time constant (τ) variations with incident light level, and we approximated the effects of irradiation by a build-up of charge near the anode contact leads. This last approximation provides a satisfactory description of the experimentally observed behavior of V_{oc} and τ .

3.0 BACKGROUND

It remains our conviction that organic-semiconductor-based photo-cells may be usefully employed as power sources in space, particularly for short-term, rapidly-assembled, low earth orbit (LEO) missions. Though they have disadvantages over classic inorganic-based cells in that their photo-conversion efficiency is low (less than 8% presently), their specific power (power per unit mass) can be substantially higher given the thin film, low mass nature of the cells. One can easily imagine their incorporation on the body of a satellite or on the surface of an inflatable, easily deployed structure. However, there have been few studies of the effects of radiation (primarily the ionizing component due to high energy protons and electrons) to which photo-cells are subjected in a LEO. For this effort we used an x-ray source to simulate the ionizing radiation in space both to characterize the induced damage and to serve as a basis for theoretical calculations of the physics of radiation damage. Therefore, this report is divided into experimental and theoretical sections, albeit overlapping.

4.0 EXPERIMENT

Early in this effort we introduced the short light pulse method¹ in which a light pulse of approximately 2 μ s duration is superimposed upon a constant but adjustable background light level. That background light is used to set the open-circuit voltage (V_{oc}) level. The short light pulse causes a small perturbation in photo-induced carrier density (Δn), which then induces a variation in V_{oc} (ΔV_{oc}). That variation subsequently relaxes in a time, τ , characteristic of the recombination of the carriers. We measured V_{oc} using a high input impedance voltmeter and $\Delta V_{oc}(t)$ using a high input impedance, digitizing oscilloscope. This method to determine τ and V_{oc} as a function of light intensity or radiation dose was employed throughout the experiments reported here.

Electron-hole pairs are generated when the cell is illuminated by a light source whose photon energy is greater than the band-gap energy. The electron-hole pair density increases with illumination time until the recombination rate equals the generation rate. In our experiments, the excess carriers were generated by a short light pulse resulting in an exponential generation and decay of excess carriers. While exposing the cells to these light pulses we measured the open circuit voltage as a function of time and used the V_{oc} rise and fall times as a measure of τ . During these experiments we observed that τ changes with excess carrier density—an observation that will be important in the following discussions.

Figure 1 shows the results of four experiments. For the first experiment we varied V_{oc} by adjusting the background light level while measuring τ . In the other three experiments V_{oc} was set to a specific value (0.34, 0.40 and 0.44 V) and τ was measured while the radiation was increased from zero to 300 krad (SiO_2). For these last three experiments τ appeared to be independent of dose. This result led us to conclude, and subsequently confirm, that there is a build-up of charge with radiation dose near the PEDOT PSS (Poly(3,4-ethylenedioxythiophene) poly(styrenesulfonate)) anode contact. And, because τ does not change with radiation dose we assume that carrier recombination is not influenced by this charge build-up.

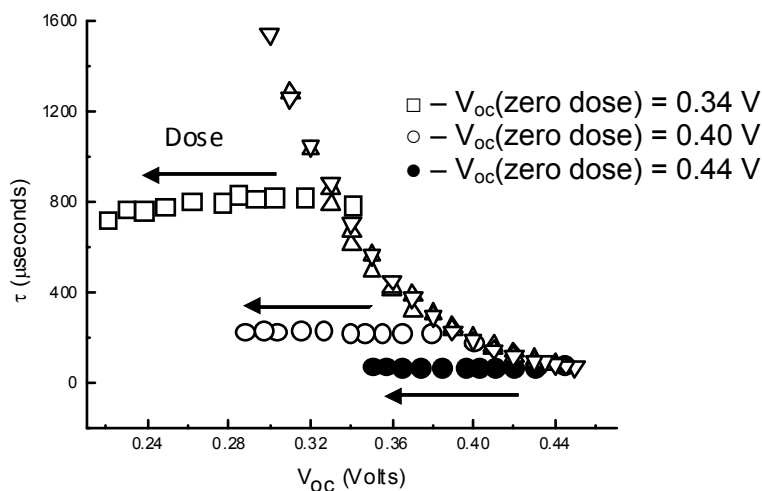


Figure 1. The effect of radiation on photo-induced carrier relaxation/recombination time constant (τ).

4.1 New Radiation Data

In view of the data shown in Fig. 1 we proceeded to adjust different variables such as the P3HT:PCBM ratio, then studied the effect of radiation for accumulated doses up to 50 krad (SiO_2) as shown in Fig. 2. The initial value of V_{oc} at dose = 0 krad (SiO_2) was the maximum value attainable for that sample with the available halogen light source. Strikingly, high weight-ratio samples appeared relatively radiation insensitive while those optimized for photo-conversion efficiency unfortunately showed a maximum for the ratios measured.

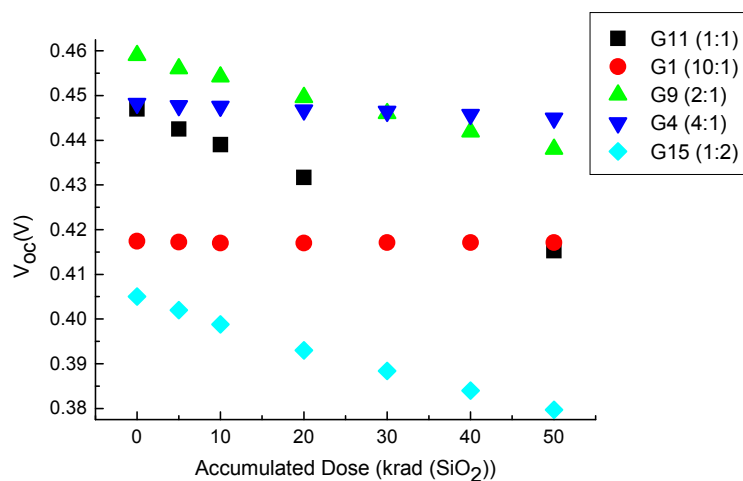


Figure 2. Effect of accumulated radiation on V_{oc} for different weight ratios of P3HT to PCBM.

Note that in Fig. 3 that the ΔV_{oc} values are shown for a total accumulated dose of 50 krad (SiO₂) and that, since the data in Fig. 2 corresponds to essentially straight line plots, one can determine the slope, $\Delta V_{oc}/\Delta Dose$ by dividing the experimental data in Fig. 3 by 50 krad (SiO₂).

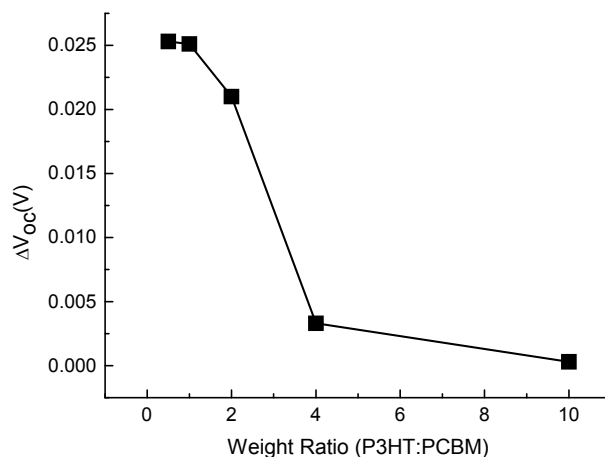


Figure 3. ΔV_{oc} plotted as a function of weight ratio.

We previously concerned ourselves with the potential issue of radiation induced charging of the glass cover slide and its possible role in inducing “effective” shifts in the V_{oc} parameter as shown in Fig. 1. Two facts now emerge to counter this possibility. First, the data in Fig. 2 is inconsistent with such a charging phenomena since all of the curves, irrespective of P3HT:PCBM weight ratio, would be expected to show some dose-dependent variation of V_{oc} and this is not the case. Furthermore we have studied dose dependence of V_{oc} in 1:1 by weight

samples having cover slides differing in thickness such that their x-ray attenuation factors differed by a factor approximately 4. For the same accumulated x-ray dose, as received by the photo-cell post attenuation, we observed the same V_{oc} variation. This eliminates the possibility of charging effects coming from x-ray absorption in the glass.

4.2 Dose Rate Effect

One of the issues that was not clear to us was whether or not different dose rates had any effect on cell charging since, as shown in Fig. 4, we have evidence for a relaxation phenomenon when irradiation is halted (times after ~ 50 minutes in Fig. 4). We will demonstrate that the presence of a relaxation term necessarily results in dose-rate dependence. Currently, V_{oc} is the observable parameter in Fig. 4, but we are more interested in the charging of the device resulting from irradiation. As an initial starting point, we assumed a first order charge generation mechanism (the first term on the right side of Eq. 1) and a simple linear relaxation term. This relation is consistent with indirect recombination in the limit of low-level injection².

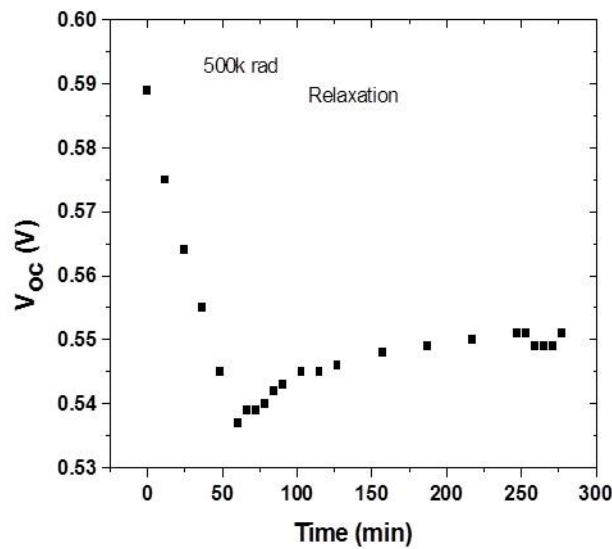


Figure 4. V_{oc} versus irradiation time up to a cumulated incident dose ~ 500 krad(SiO₂). Subsequently the device was allowed to relax ($t > 50$ min).

$$\frac{dP(t)}{dt} = D\sigma_p\varphi(P_0 - P) - kP \quad (1)$$

This yields the following solution for the evolution of the charge density as a function of time:

$$P(t) = \frac{D\sigma_p\varphi P_0}{D\sigma_p\varphi + k} (1 - e^{-(D\sigma_p\varphi + k)t}) \quad (2)$$

In this last equation $P(t)$ is the trapped charge concentration, D is the dose rate, σp is the charge capture cross section (neutral traps), ϕ is the electron-hole escape probability, P_0 is the maximum density of traps, and k is a relaxation parameter. Equation 2 suggests that there is dose-rate dependence through two factors: a) if $k > D\sigma p\phi$ or $k \sim D\sigma p\phi$, then the saturation level is less than P_0 and is reduced to $D\sigma p\phi P_0/k$ for those instances in which $k \gg D\sigma p\phi$ and b) the initial slope ($dP/dt |_{t \rightarrow 0}$) is equal to $D\sigma p\phi P_0$. To investigate this, different dose rates were used with 1:1 devices. Figure 5 shows the relationship between V_{oc} and accumulated dose for different dose rates in these 1:1 samples. This analysis assumes linearity and constancy of coefficients in the linear ordinary homogeneous differential equation. We approximated ΔV_{oc} as ΔP , although this assumes a constant coefficient linear relationship between charge density and V_{oc} which is not necessarily correct. This point will be addressed later.

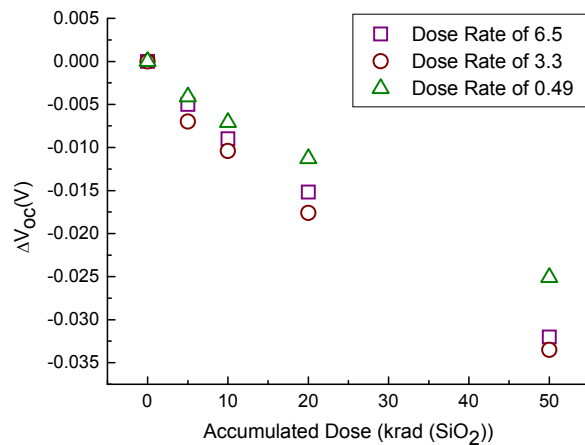


Figure 5. ΔV_{oc} plotted as a function of accumulated dose for 1:1 samples. Attenuation factor is being accounted for in the dose rates. All dose rates are in krad/min (SiO₂).

From Fig. 5 it would appear that there is some dose-rate effect on ΔV_{oc} —although not a linear function of dose rate as we might have anticipated. However, it must be noted that we were very limited in terms of the lowest dose rate we could use. For example, the data taken using a dose rate of 0.49 krad (SiO₂) required the x-ray machine to function for more than 100 minutes, which is not desirable. Using a higher dose rate did not produce abnormal effects on V_{oc} and the results were about the same as when the dose rate was 7.3 krad/min (SiO₂). However, we believe that the change in V_{oc} will reach a saturation limit at higher dose rates. This could explain why the change in V_{oc} was slightly higher for the 3.3 krad/min (SiO₂) dose rate than for the 6.5 krad/min (SiO₂) dose rate. Another cause could be noise in the experiment.

4.3 Relationship between Charge and Accumulated Dose

As mentioned previously, we plotted ΔV_{oc} as a function of dose in Fig. 5 but would have preferred to plot charge density as a function of dose. Using theoretical modeling (to be discussed) we can translate V_{oc} into a charge density and re-plot Fig. 5 as Fig. 6. A linear relationship between charge density and accumulated dose appears, showing that the approximate form used to generate Fig. 5 was adequate.

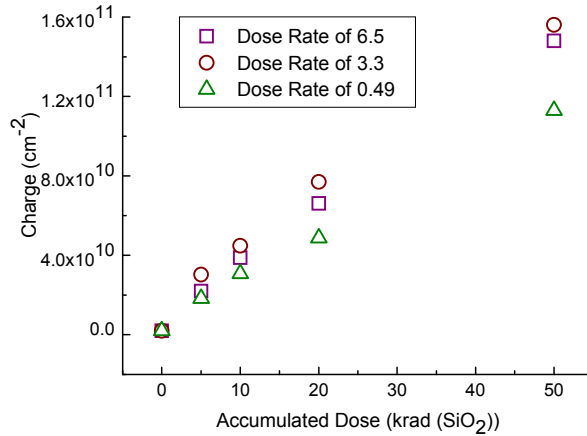


Figure 6. Charge plotted as a function of accumulated dose.

4.4 Ancillary interface modification studies

We previously attributed variations in V_{oc} in 1:1 samples as being due to charge buildup at the anode interface. We also carried out experiments on 1:1 samples in which the cathode interface was modified by addition of thin films of ZnO, LiF, TiO_2/Cs , and standard Ca/Al or pure Al. These cells were again subjected to varying levels of optical irradiation from a halogen lamp and the voltage relaxation time was measured versus V_{oc} (see Fig. 7).

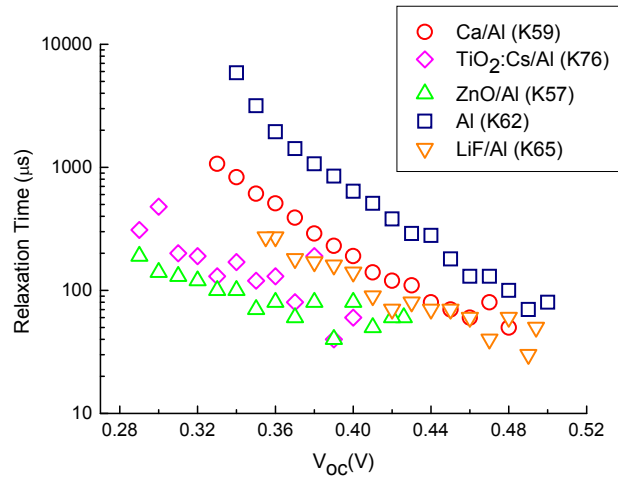


Figure 7. Experimental results of the relaxation time measurements (logarithmic scale) of 1:1 P3HT: PCBM samples with different interfaces at the cathode.

Following Koster³, et al., one can express τ in the form:

$$\tau = \tau_0 e^{-\frac{qV_{oc}}{kT}}, \text{ where } \tau_0 = \frac{L_{eff}}{q D} \frac{1}{\gamma N_D^2} \quad (3)$$

where q is the elementary charge, k the Boltzmann constant, T the temperature, E_{gap} is the energy difference between the highest occupied molecular orbital (HOMO) of the electron donor and the lowest unoccupied molecular (LUMO) of the electron acceptor, γ the recombination constant, and N_c the density of states in the conduction band. From this expression we anticipate a linear relationship between $\ln(\tau)$ and V_{oc} with a slope of $-q/kT$ and this should be independent of the interface. This is clearly not the case, indicating that modification of the cathode interface varies the exponential factor which should, in fact, be a constant. At the present time we have no explanation for this phenomenon but hope that theoretical modeling will provide some insight. Irradiation studies of these interface-modified systems should also help explain the phenomenon.

5.0 MODELLING

In the following sections we describe our efforts to model the effects observed experimentally.

5.1 Simulations (General Information)

To simulate the organic photocells we used device simulation software designed for conventional semiconductors such as silicon and gallium-arsenide (GaAs). Two codes were used: Radiation Effects in Oxides and Semiconductors (REOS)⁴ (developed at Sandia National Laboratories) and Silvaco Atlas⁵ which is a commercial device simulation code. Silvaco Atlas works by solving the drift-diffusion equation and Poisson equations simultaneously in order to predict the carrier densities and potentials within the device under known biasing. It then uses those values to calculate the current.

For our initial approach we used REOS to model the organic solar cell as a layered PN junction similar to a silicon solar cell but with changed physical parameters to represent the lower mobilities and different band gap of the materials. This approach, however, is physically incorrect since the blended organic material is not two distinct layers with high doping. Later we switched to Silvaco based on an already implemented Langevin recombination model and the advantage of highly-debugged commercial code.

Presently, the device is modeled as a photovoltaic device that is 200 nm thick, with an effective area of 2 mm by 1 mm or 2 mm². To accomplish the simulation in Silvaco, the device structure is modeled as a continuous device with uniform cross section from the cathode, through the PCBM:P3HT (also termed the blend) to the PEDOT, (which functions as the anode) with no variations in the blend or the cross sectional area. The blend is treated as a single material with a single set of physical parameters in which a built-in potential is created by the work functions of the two contacts—similar to the method used in Reference 6. The cathode is presently assumed to be aluminum and the effective work function of the PEDOT is chosen so that the lifetime vs. open-circuit voltage predicted by Silvaco is close to that measured experimentally. This results in a work function difference of 0.9 Volts. Unlike some work by others, rather than injecting excitons, our simulations inject only free electron-hole pairs. However, this seems unlikely to be a major approximation.

5.2 Open-circuit voltage simulations (Pre-radiation)

To determine the open-circuit voltage for a given electron-hole (e-h) pair generation rate, we set a zero-current boundary condition on one of the contacts then calculated the resulting potential on that contact. The zero current boundary condition is a goal which the code attempts to achieve, and is allowed to approach to within a certain precision. The resulting current is actually very small rather than zero. We made several calculations under these conditions and incorporating various combinations of Langevin and Shockley-Reed-Hall (SRH) recombination, including both and neither. (The carrier lifetimes that are calculated when both Langevin and SRH recombination are turned off are due to the field driving the carriers to the contacts where they recombine, an obviously ideal situation.) The goal was to determine the dominant recombination method. The most surprising result of this simulation was that the predicted open-circuit voltage was only slightly affected by the inclusion of Langevin recombination as can be seen in Fig.8. The inclusion of SRH recombination along with Langevin caused a displacement of the curve and a different slope similar to the results seen by Mandoc⁷. In comparing these results to the Langevin formalism used by others it is worth noting that V_{oc} is still linearly dependent on the log of the generation rate. The conclusion of these simulations is that for the relatively thin samples upon which this effort was based, neither SRH nor Langevin is the dominant recombination mechanism when the density of SRH recombination centers is low, that the carrier recombination follows with the density of SRH recombination centers, and finally that Langevin recombination does not play a role in carrier recombination.

5.3 Relaxation Time Simulations (Pre-radiation)

In order to simulate the experimental extraction of e-h lifetime we initially we used a step function in which the e-h generation rate dropped from a high value to a low value. This is in contrast to the experiment in which a constant light is shown on the switch and a pulse of light is added and removed. While this step approach produced reasonable results, we decided to simulate the pulse nature of the experiment.

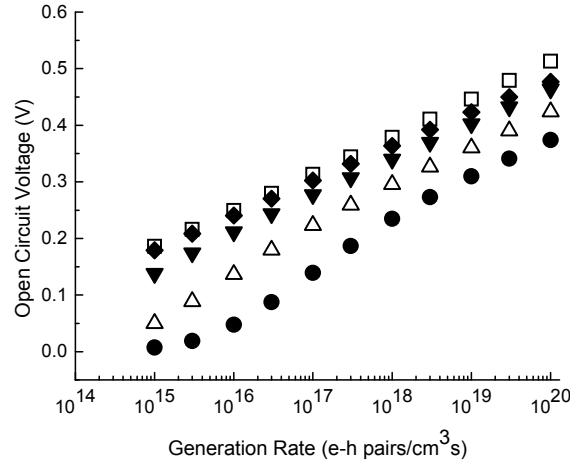


Figure 8. Predicted V_{oc} as a function of the carrier injection rate for different recombination methods; (□) no SRH or Langevin, (◆) Langevin only, (▼) $\tau_{SRH} = 10^{-6}$ s, (Δ) $\tau_{SRH} = 10^{-7}$ s, and (●) $\tau_{SRH} = 10^{-8}$ s.

At a chosen e-h generation rate, which corresponds to a chosen illumination level, we ran the simulation until steady state was achieved. We then applied a short duration (2 μ s) pulse and extracted the lifetime (τ) from the behavior of V_{oc} after the pulse ended. The height of the pulse was chosen so that ΔV_{oc} caused by the pulse was similar to the experimental value at $V_{oc} \sim 0.004$ Volts.

As seen in Fig. 9, inclusion of Langevin recombination again had a small effect on the extracted lifetimes and slope of $\ln(\tau)$ vs. V_{oc} . Thus, without any SRH the slope was approximately -34.5. According to the Langevin analysis from Eq. 3, the slope is $-kt/q \cong -38.6$ while the experimental values depend on the cathode interface and range from 26.5 to 38.6. The inclusion of SRH recombination changed not only the magnitude of τ but also the slope of the $\tau(V_{oc})$ curves, lowering them to as little as -22.7 when the lifetime was 10^{-8} s. While the traps in these simulations were placed uniformly in the device, it is possible to explain the experimental change in the slope of the lifetime curves as being due to different trap densities and, therefore, SRH lifetimes.

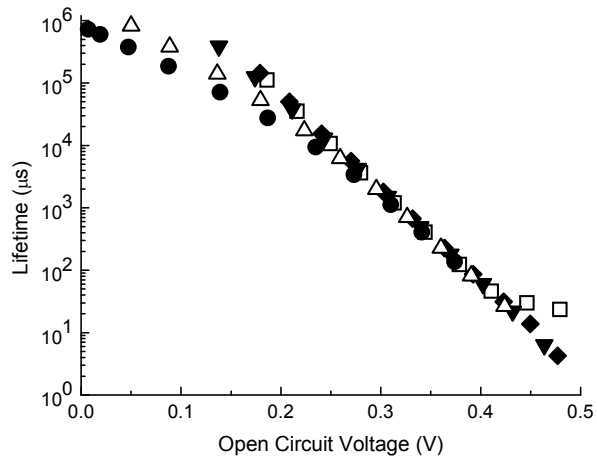


Figure 9. The lifetime as a function of V_{oc} for different recombination methods; (□) no SRH or Langevin, (◆) Langevin only, (▼) $\tau_{SRH}=10^{-6}$ s, (Δ) $\tau_{SRH}=10^{-7}$ s, and (●) $\tau_{SRH}=10^{-8}$ s.

5.4 Charging Simulations

In order to test our hypothesis that the experimental irradiation results, in which V_{oc} dropped as τ remained constant, was due to the buildup of trapped charge, we included a small region of trapped holes near the simulated anode. We increased this trapped charge level to simulate the effect of having a greater total dose. The qualitative matching was good as shown in Figures 10 and 11. In Figure 11, the open circuit voltage follows the solid curve with triangles from the upper left to lower right as the light level is increased. In other words, light level is the parameter for this curve. Further, the curve shows that as the light induced open circuit voltage is increased, the carrier lifetime is reduced. To simulate an experiment, a light level is set, which places the start of a simulation at a particular point along this curve, and is the initial point for the simulation. A simulated radiation is applied by increasing the trapped hole density near the anode, causing the open circuit voltage to drop from the initial point as shown in Figure 11. These simulations are shown in Figure 11 with open squares, open and closed circles. One can readily see that while the open circuit voltage drops, the lifetime as a function of simulated dose is flat, up to a point, at which point all three curves have notable upswings at low biases. At present it is not clear if this is an artifact of the calculation or something real which could be seen experimentally if the total dose were high enough.

From the same simulations we were able to link the level of the charging to the effect that the charging had on V_{oc} . The three initial biases represented in Fig. 11 all have similar values for charging below $3 \times 10^{12} \text{ cm}^{-3}$, and begin to spread apart at higher densities. These higher densities correspond to the upswing at low V_{oc} .

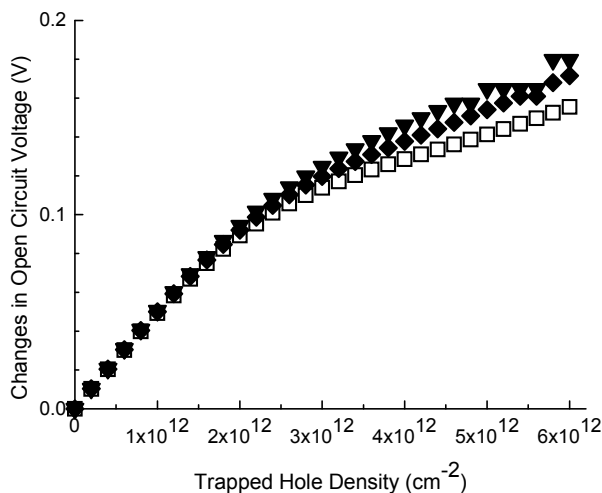


Figure 10. The simulated change in V_{oc} due to the presence of the trapped hole density; (□) the V_{oc} with zero charge is 0.33 V, (○) 0.40 V, and (●) 0.45 V.

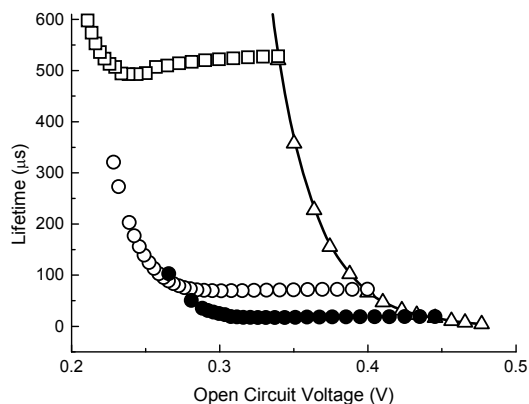


Figure 11. The simulated carrier relaxation time as a function of V_{oc} : (Δ) the incident light level was adjusted to vary V_{oc} , (□, ○, and ●) increasing trapped hole density near the anode with the initial V_{oc} =0.33V, 0.40V, and 0.45 V respectively.

6.0 Conclusions

This effort was initiated at the request of AFOSR with the goal of determining the effect of radiation upon the performance of organic semiconductor devices. The results of this experimental and modeling effort were then to be transitioned to organic device investigators for use in developing mitigation techniques. The findings included the discovery that while carrier

lifetimes were unaffected by ionizing radiation, degradation did occur and manifested itself in the development of an internal potential that tended to reduce efficiency of the organic photovoltaic devices tested.

The team recommends additional modeling and experimental efforts to answer questions that arose. Specifically, was the upswing in carrier lifetimes at high total integrated dose levels real or an artifact of the simulation. Additionally, we recommend taking a further step by integrating “real” space conditions into our experiments and utilizing ultra-low dose rates (1 rad/min (SiO₂)). Application of realistic dose rates will enable a better understanding of the effects of radiation on the solar cells and will be more representative of what might happen if the cells are sent to space. We also recommend investigating the device parameters that change due to radiation. This also includes a deeper look into the changes in the shunt and series resistances, and the ideality factor will help understand the physics behind the cells.

There are several more questions to answer, for which the simulations will need to be improved. The experimentally-extracted lifetime rises as the open circuit voltage falls but reaches a saturation lifetime in the limit of low initial V_{oc} . Currently our simulations have not been able to recreate this saturation. It is possible that a different kind of recombination than either Langevin or SRH is present. If so, the lifetime will not depend on V_{oc} , or by extension, the carrier densities since the carrier densities depend on the field and V_{oc} . It is also worth noting that device simulators have some difficulty accurately predicting results when light intensities are low. Secondly, the sensitivity of the parameters of an organic solar cell with X-ray bombardment to the ratio of the P3HT:PCBM should be explored. At present no modeling has explained the observed sensitivities. Further expansion of the simulations is necessary.

References

1. G. Shuttle, B. O'Regan, A. M. Ballantyne, J. Nelson, D. D. Bradley, J. de Mello and J. R. Durrant, "Experimental determination of the rate law for charge carrier decay in a polythiophene:Fullerene solar cell," *Appl. Phys. Lett.*, **92**, 093311-1-3, 2008.
2. E. S. Yang, "Microelectronic Devices," McGraw Hill, 1988.
3. L. J. A. Koster, V. D. Mihailetschi, R. Ramaker and P. W. M. Blom, "Light intensity dependence of open-circuit voltage of polymer: fullerene solar cells," *Appl. Phys. Lett.*, **86**, pp. 123509-1-3, 2005.
4. H.P. Hjalmarson, R.L. Pease, S.C. Witczak, M.R. Shaneyfelt, J.R. Schwank, A.H. Edwards, C.E. Hembree and T.R. Mattsson, "Mechanisms for radiation dose-rate sensitivity of bipolar transistors," *IEEE Trans. Nucl. Sci.*, **50**, 1901 (2003).
5. "ATLAS user's manual, Device simulation software," SILVACO International (2007).
6. I. Hwang and N. C. Greenham, "Modeling photocurrent transients in organic solar cells," *Nanotechnology*, **19**, 424012 (2008).
7. M. M. Mandoc, F. B. Kooistra, J. C. Hummelen, B. de Boer and P. W. M. Blom, "Effect of traps on the performance of bulk heterojunction organic solar cells," *Appl. Phys. Lett.*, **91**, 263505-1 (2007).

DISTRIBUTION LIST

| | |
|--|-------|
| DTIC/OCF 8725 John J. Kingman Rd, Suite 0944 Ft Belvoir, VA 22060-6218 | 1 cy |
| AFRL/RVIL Kirtland AFB, NM 87117-5776 | 2 cys |
| Official Record Copy AFRL/RVSE/Clay Mayberry | 1 cy |